Independent anatomical and functional measures of the V1/V2 boundary in human visual cortex

Holly Bridge
University Laboratory of Physiology, University of Oxford, Oxford, UK

Stuart Clare
Oxford Centre for Functional Magnetic Resonance Imaging of the Brain, Department of Clinical Neurology, University of Oxford, Oxford, UK

Mark Jenkinson
Oxford Centre for Functional Magnetic Resonance Imaging of the Brain, Department of Clinical Neurology, University of Oxford, Oxford, UK

Peter Jezzard
Oxford Centre for Functional Magnetic Resonance Imaging of the Brain, Department of Clinical Neurology, University of Oxford, Oxford, UK

Andrew J. Parker
University Laboratory of Physiology, University of Oxford, Oxford, UK

Paul M. Matthews
Oxford Centre for Functional Magnetic Resonance Imaging of the Brain, Department of Clinical Neurology, University of Oxford, Oxford, UK

The cerebral cortex has both anatomical and functional specialization, but the level of correspondence between the two in the human brain has remained largely elusive. Recent successes in high-resolution magnetic resonance imaging of myeloarchitecture patterns in the cortex suggest that it may now be possible to compare directly human anatomy and function in vivo. We independently investigated the anatomical and functional borders between primary and secondary human visual areas (V1 and V2) in vivo. Functional borders were mapped with functional magnetic resonance imaging (fMRI) using a narrow, vertical black and white contrast-reversing wedge. In three separate scanning sessions, anatomical images were collected at three different slice orientations (300 μm x 300 μm, slice thickness, 1.5 mm). The anatomical signature of V1 was determined by the presence of a hypointense band in the middle of the cortical gray matter. The band was identified in between 81% and 33% (mean 57%) of V1 defined using fMRI, and less than 5% of the identified band was in cortex outside V1. Intensity profiles taken through the gray matter on the V1 and V2 sides of the functional border indicate a measurable difference in the size of the hypointense band for all subjects. This is the first demonstration that the definition of V1 by fMRI closely matches the anatomically defined striate cortex in the human brain. The development of very high-resolution structural MRI may permit the definition of cortical areas based on myeloarchitecture when functional definition is not possible.

Keywords: primary visual cortex, high-resolution MRI, myeloarchitecture, stria of Gennari

Introduction

The addition of functional magnetic resonance imaging (fMRI) to the range of neuroscience techniques has allowed new insights into the functioning of the human brain. However, it has also led to methodological challenges not present when using nonhuman species. The inability to use histological techniques means that the loci of activity in different subjects can only be compared approximately based on stereotaxic coordinates. Such an approach is limited by the significant variation between subjects in brain size, shape, and the precise location of cortical areas (Amunts, Malikovic, Mohlberg, Schormann, & Zilles, 2000; Andrews, Halpern, & Purves, 1997; Dougherty et al., 2003; Stensaas, Eddington, & Dobelle, 1974).

A more reliable approach is to produce an independent definition of a brain area, either anatomical or functional, and then measure the neural response in a particular experiment in that predefined region. Leading in the use of this methodology are the visual scientists. By exploiting the separate retinotopic map in each of the early visual areas, it is possible to functionally predefine up to six or seven cor-

doi:10.1167/5.2.1 Received June 18, 2004; published February 11, 2005 ISSN 1534-7362 © 2005 ARVO

tical areas (DeYoe et al., 1996; Dougherty et al., 2003; Engel, Glover, & Wandell, 1997; Engel et al., 1994; Hadjikhani, Liu, Dale, Cavanagh, & Tootell, 1998; Sereno et al., 1995; Wade, Brewer, Rieger, & Wandell, 2002). These functional definitions have been used to measure the sizes of V1, V2, and V3 in human visual cortex, and give similar results to many anatomical studies (Dougherty et al., 2003).

Although widely used, it has not been possible to measure, for an individual subject, how these functionally defined visual areas compare to anatomically defined regions of occipital cortex. The striate cortex, or Brodmann's area 17, occupies a large region of the occipital lobe along the calcarine sulcus. It can be distinguished from neighboring regions by the presence of the stria of Gennari, a thick band of myelination in layer 4B. Although this myeloarchitecture has been identified in postmortem tissue for over two centuries (Gennari, 1782), it is only recently that visualization has become possible in vivo. Several groups have now used human MRI to image the visual cortex at high resolution to identify the stria of Gennari (Barbier, et al., 2002; Clark, Courchesne, & Grafe, 1992; Walters et al., 2003). Of these studies, only Walters et al. (2003) attempted to make any comparison between anatomically defined cortical myeloarchitecture and functional activity. They showed that a region with a myelination pattern similar to the middle temporal area (MT) in the macaque lay within an area of the occipital lobe that showed significant activity to moving, compared with stationary stimuli. However, the human MT complex (responsive to such stimuli) is believed to consist of multiple visual areas (Huk, Dougherty, & Heeger, 2002; Tootell & Taylor, 1995; Watson et al., 1993; Zeki et al., 1991). In contrast, the clear retinotopic map of V1 allows a direct comparison between this area defined functionally using the retinotopic mapping technique and anatomically by the presence of the stria of Gennari.

The correspondence between anatomical and functional definitions of V1 is difficult even for invasive animal studies. First, this is because there is no definitive test to distinguish between neuronal responses in V1 and V2, and, second, because the receptive fields in both areas have very similar spatial locations in the region of the border. It is this latter feature that was exploited by Zeki (1970) to demonstrate correspondence in the macaque monkey. The vertical meridian is represented at the border between V1 and V2; therefore, it is necessary to have some information shared across the corpus callosum. By sectioning the splenium, Zeki showed that the region between areas 17 and 18 (V2) exhibited degeneration that extended approximately 0.5 mm into layer IV of the striate cortex. The extent of the degeneration on the area 18 side of the boundary is not stated.

Here we use MR imaging to identify myelination patterns within the cortical gray matter of the occipital cortex to investigate the correspondence between the anatomical and functional border between V1 and V2. The approach that we adopted was designed to be analogous to the degeneration study of Zeki. Using a narrow flashing wedge, we functionally mapped the vertical meridian in five subjects, and compared the location of the resulting activation to the areas in which striated cortex could be identified.

To demonstrate correspondence, it is necessary to show that (i) striated cortex is found in a large proportion of the functionally defined V1, (ii) little or no striated cortex is found outside of functionally defined V1, and (iii) in the area surrounding the V1/V2 border, regions on the V1 side of the border have a significantly larger dip in intensity (indicating the presence of myelination) compared to regions on the V2 side.

This is the first anatomical verification of the functional mapping of human visual areas using MRI. Although the surface area of functionally defined V1 in which striated cortex could be identified varied considerably across subjects (33-81%), very little striated cortex was found outside the border region.

Methods

Magnetic resonance data were acquired on a 3T whole-body scanner (Varian Unity Inova, Palo Alto, CA), with a head insert gradient coil (Magnex, Oxford, UK) giving a maximum gradient strength of 34 mT/m. Five subjects aged 24-31 years (2 male) with normal or corrected-to-normal vision each participated in five scanning sessions.

Anatomical data collection

High-resolution images were acquired using a four channel receive-only surface array coil (Nova Medical, Wakefield, MA). In three separate scanning sessions, we collected data at three different orientations: midline sagittal, parallel, and perpendicular to the calcarine sulcus. Either 16 (parallel to calcarine sulcus) or 32 slices (1.5 mm thick) were scanned at an in-plane resolution of 300 μm x 300 μm (matrix size 384 x 512). A 120° preparation pulse was followed 300 ms later by a train of 20° excitation pulses (TR = 30 ms, TE = 11 ms). There were no steady state pulses in this train and k-space coverage was center out. In each session, either 10 (for 32 slice scans) or 12 repeats were performed, each linearly registered to the first using FLIRT (Jenkinson, Bannister, Brady, & Smith, 2002) and averaged.

A whole brain T1-weighted image was collected in an additional scanning session using a brain volume coil (Varian, Palo Alto, CA). Axial slices, 1-mm thick, were acquired at a resolution of 1 x 1 mm^2. These anatomical images were automatically segmented into gray and white matter using FAST (Zhang, Brady, & Smith, 2001), and manually refined using custom software from Stanford University (Teo, Sapiro, & Wandell, 1997). Segmented gray matter was computationally flattened for displaying data and making comparisons between anatomical data and regions of functional activation (Wandell, Chial, & Backus, 2000).

Stimuli

Stimuli were presented on a VSG 2/5 graphics card (Cambridge Research Systems, Cambridge, UK) using an XGA projector (Sanyo, Watford, UK) directed down the center of the bore to a small screen attached to the scanner. The screen was viewed by the subject from a distance of approximately 0.4 m through small mirrors above their head. This arrangement gave a visual field between 15° and 20° high, depending on the size of the subject

The wedge consisted of black and white contrast reversing squares (shown in Figure 3). Its polar angular extent was 8° into each hemifield such that 4.4% of the total visual field was stimulated during an "on" period. The stimulus was designed to activate regions of cortex similar to those that degenerated in the study of Zeki (1970) (i.e., those that represent the vertical meridian). However, the stimulus extent was increased beyond the 2-3° necessary for this to ensure that activation levels reached statistical significance in all subjects. The stimulus was presented in a block design alternating with a blank screen (32-s period). To maximize the extent of the functional activation, separate scans were performed while subjects' fixation was directed either up or down, such that the stimulus extended into the lower or upper visual field.

In addition to mapping the vertical meridian, we performed standard retinotopic mapping in an additional scanning session for each subject. The angular dimension was mapped with a 45° rotating wedge that was advanced by 30° every TR (4 s). An expanding ring stimulus was used for mapping eccentricity. Both stimuli were constructed from a black and white dartboard contrast reversing at 8 Hz. The resulting retinotopic maps were used to objectively measure the location of the V1/V2 border using the semi-automated method of Dougherty et al. (2003). This method simultaneously fits an expected pattern of activation to both the eccentricity and angular retinotopic maps, and is explained in more detail in Dougherty et al.

FMRI data collection and analysis

Echo planar images (EPI), oriented perpendicular to the calcarine sulcus, were acquired with a quadrature surface coil (NOVA Medical, Wakefield, MA) using typical parameters (TR = 4 s, TE = 30 ms, 2.0 x 2.0 mm in-plane resolution, thirty-two 2-mm slices). Each scan consisted of 6 blocks, giving a total scan length of 192 s. Ten scans were performed in total, 5 with upper and 5 with lower fixation. At the end of this session, a T1-weighted image with the same slices as the functional data was collected to aid alignment to the whole brain anatomical image.

The first stimulus cycle of each scan was discarded to minimize transient effects of signal saturation. The linear trend in the time series at each voxel was removed to compensate for slow signal drift (Smith et al., 1999). Time series for the five repeats of each stimulus type were then averaged.

To investigate the areas of cortex activated by the stimulus, a Fourier analysis was performed on the data. The response coherence (amplitude at stimulus frequency divided by the summed amplitudes at all frequencies) was used as a threshold measure, and p values were obtained via a Fisher transform of the correlation coefficients. The phase of the activity was also restricted to within $\pi/2$ of the stimulus presentation phase.

Analysis

The three very high-resolution images were aligned to the whole brain T1-weighted 1 x 1 x 1 mm^3 using a semi-automated 3D coregistration algorithm (Nestares & Heeger, 2000). Functional data were also transformed into this whole brain space for comparison.

Identification of cortical striation

Three observers independently identified all regions on the very high-resolution images in which they could visualize a hypointense band within the cortex. Using MRIcro (www.MRIcro.com), a single pixel line was drawn over this region. This region of interest (ROI) was then dilated to a thickness of 2 mm, approximately equal to the cortical thickness. A region of cortex was defined as having cortical striation if it was identified by at least two of the three observers as defined by the intersection of these dilated ROIs. Cortical striation from the three different scanning orientations were transformed into whole brain space and combined to give a total volume of cortical striation for each subject. To ensure that no observer was biasing the sample by consistently identifying larger regions of striated cortex, we performed a two-way ANOVA on the number of pixels selected, and found no effect of observer ($F = 0.14$, $p > .8$, d.f. = 2).

Grey matter intensity profiles

Manual identification of myelination patterns does not allow objective measurement of the intensity changes associated with the presence of myelination. To obtain a more objective measurement of these changes, we took intensity profiles across the cortex. To achieve this, regions of cortex were selected by a single pixel line parallel to and in the middle of the gray matter. Profiles perpendicular to that line were then calculated for each voxel (except the end points) and averaged to give a mean intensity profile for regions of V1 and V2 in each subject. To quantify differences between V1 and V2 intensity profiles, each profile was detrended and the difference between maximum and minimum values calculated. A t test was performed to test for significant differences between the values for V1 and V2 profiles.

Results

Regions in which the cortical striation could be identified were apparent at all slice orientations in all subjects. The left column of Figure 1 shows an example of a single

slice imaged at 300 μm x 300 μm perpendicular to the calcarine sulcus for each of the five subjects. In these images white matter is dark, and the striated cortical regions can be visualized as having a hypointense band within the gray matter. In all subjects, the striation is most evident in the calcarine sulcus. This can be seen more clearly in the right column of Figure 1, which shows the region around the calcarine sulcus. Although the images oriented perpendicular to the calcarine sulcus contained the most cortical striation in 4/5 subjects, it was also evident in both the other orientations. Figure 2 shows a slice scanned parallel to the calcarine sulcus (lower row) and a slice from a midline sagittal scan. In this subject (Subject 1), the cortical striation can be seen in extended regions of gray matter in the magnified views. In general though, the data from these slice orientations showed less cortical striation than found in the coronal orientation.

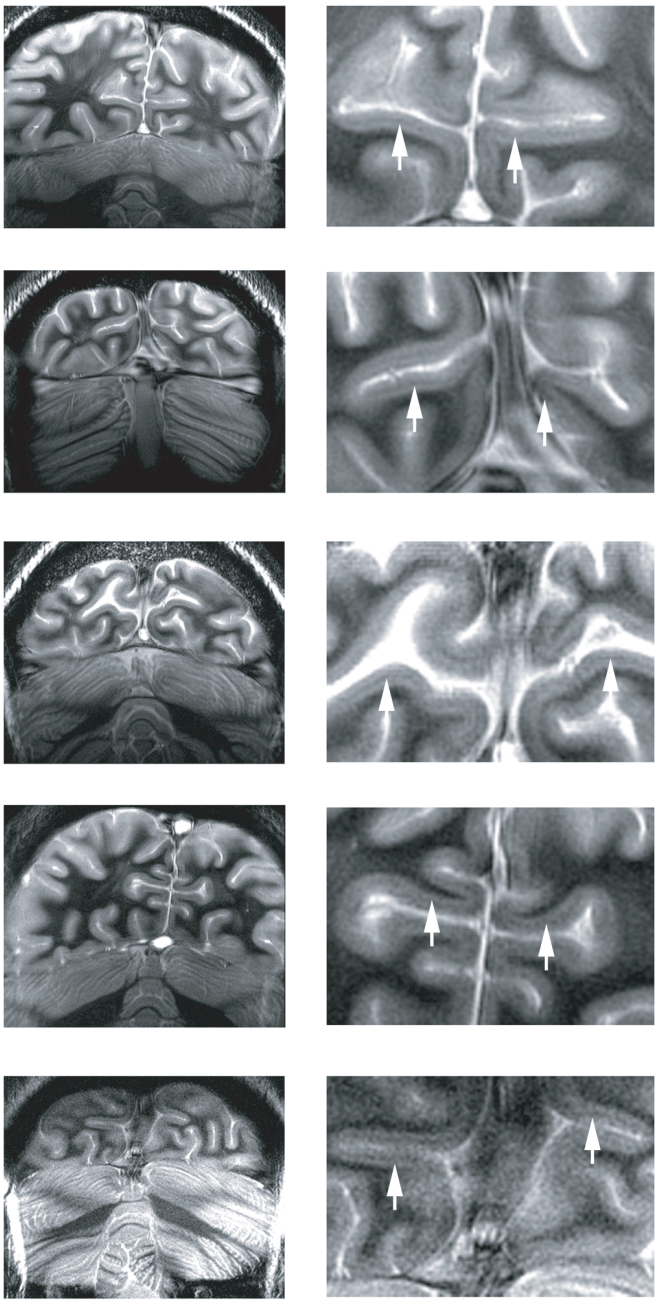

Figure 1. Single slices from high-resolution images for the five subjects. The left column shows slices oriented perpendicular to the calcarine sulcus. The images on the right show the region in the white boxes at greater magnification. Cortical striation can be seen in all subjects as a dark line within the calcarine sulcus (indicated by the white arrows). This striation is evident in multiple slices.

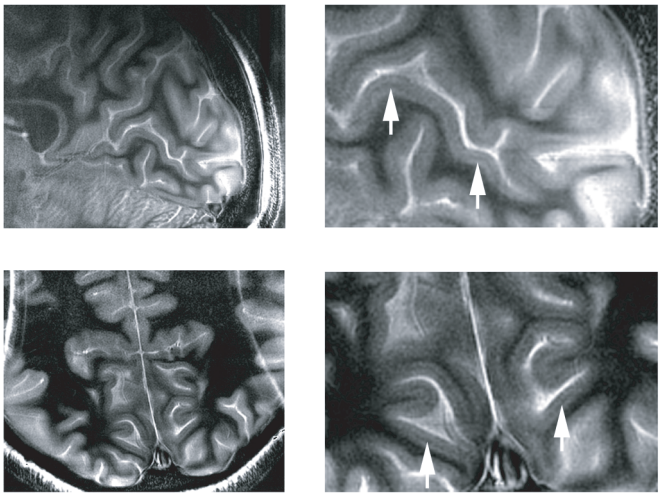

Figure 2. Additional slice orientations used for visualizing the cortical striation of the occipital lobe. The upper row shows an example of a midline sagittal slice, and the lower is a slice oriented parallel to the calcarine sulcus. Extended regions of gray matter containing striation can be seen in both examples (data from Subject 1).

Functional boundary between V1 and V2

The functional border between V1 and V2 was located using a 16° wedge centered on the vertical midline (extending 8° into each hemifield), as shown in Figure 3A. Also shown is an example of the functional activity overlaid on the left hemisphere for Subject 1. On these flattened representations, darker regions represent sulci and light gray regions are gyri. The calcarine sulcus is located at the center of these maps. Functional activity is shown for response coherence values > 0.3 and activity phases within $\pi/2$ of the stimulus presentation period. The displayed MR signals range from a threshold of $p > .01$ (cyan) to a maximum of $p > 10\text{–}8$ (magenta, uncorrected). The activity can be seen as lines on the flat surface as predicted by retinotopic mapping. The boundary between V1 and V2, defined with retinotopic mapping using the automated method of Dougherty et al. (2003), is shown in red.

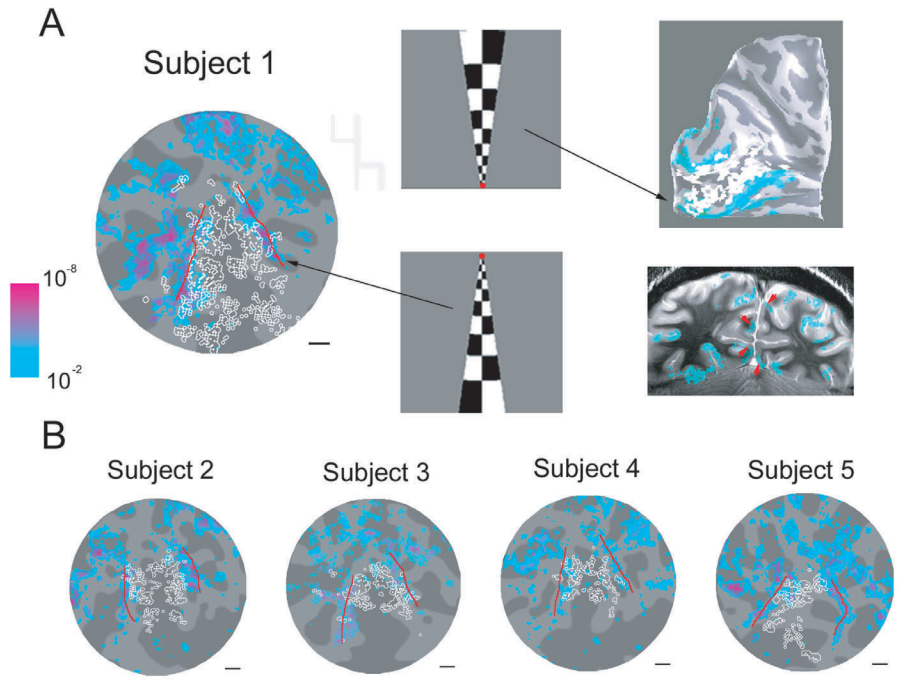

Figure 3. Flattened representations of the occipital lobe showing functional and anatomical data. A shows a pictorial representation of the stimulus used for mapping the vertical meridian. On the left is a computationally flattened occipital lobe (left hemisphere) in which dark gray areas represent sulci, and light gray areas gyri. The calcarine sulcus is at the center of the flat map. The functional activation in response to stimulation of the vertical meridian is shown for p values ranging from $p > .01$ (cyan) to $p > 10^{-8}$ (magenta) as shown by the scale. Superimposed on this activation map in a white outline are the gray voxels in which cortical striation has been identified. The red line indicates an objective measure of the V1/V2 boundary from retinotopic mapping, collected independently of the meridian fMRI data shown. The upper right panel shows the region of functional activation (cyan) and the striated cortex (white) transformed onto a three-dimensional rendering of the occipital lobe, and the lower right shows the regions of functional activation on a high-resolution anatomical image slice. B shows the data from the right hemisphere of each of the other four subjects. In each case, the scale bar represents 10 mm.

The striated cortex, identified from the high-resolution anatomical images, is shown in white, and in this subject (Subject 1) covers 81% of the functionally defined V1. To allow the localization of these regions of activity on the cortical surface, both the functional activation (cyan) and anatomically defined striated cortex (white) are shown on an inflated rendering of the left occipital lobe (top right). This clearly shows the majority of the cortical striation lying within the calcarine sulcus, although less striated cortex, is present deep in the sulcus. The bottom right panel shows a rendering of the functional data on a single slice of a very high-resolution scan. The arrows point to the functional activity located at the V1/V2 border.

Figure 3B shows the right hemisphere for each of the other four subjects. For each subject, it is possible to functionally define the V1/V2 boundary along a large section of the calcarine sulcus. To demonstrate anatomical and functional correspondence, it is necessary to show that the region functionally identified as V1 contains a large area of striated cortex, and that very little striated cortex lies outside this region. As can be seen from the flattened representations, the amount of anatomically defined striated cortex varies considerably between the five subjects. In the area of functionally defined V1 that was scanned in all three anatomical scans, the percentage coverage with striated cortex (both hemispheres) varies from 81% to 33% (Subject 1, 81%; Subject 2, 68%; Subject 3, 40%; Subject 4, 64%; and Subject 5, 33%). Possible explanations for this large intersubject variation in coverage are discussed later.

In the region outside of the functionally active border region, small patches of striated cortex can be seen for Subjects 1, 3, and 4. In fact, such areas can be seen in 6 of 10 hemispheres. These small "extra-striate" patches never accounted for more than 5% of the total striated cortex detected though.

It is clear from these data that the anterior extent of the anatomically defined striate cortex is greater in some cases than the functionally defined border. However, this is a consequence of the limited visual field available within the scanner (15-20°), which means that regions of cortex representing more eccentric areas of space are not activated by the stimuli.

Objective measurement of intensity changes through the cortex on anatomical images

To measure the intensity changes through the cortical gray matter, we took the mean of multiple cross-sections through the cortical layers. In regions where striated cortex has been identified, an intensity profile should show a dip around the middle of the gray matter. To measure the difference in intensity profile between the V1 and V2 sides of the functional boundary, profiles were taken immediately adjacent to the active regions, as shown in Figure 4A. The regions identified in the flattened space were transformed back into the high-resolution anatomical space, and a V1 and V2 region was defined in multiple slices by a single pixel ROI line through the center of the gray matter. An automated procedure calculated profiles perpendicular to this ROI line in each slice. Due to the difficulty in this calculation at areas of high curvature, both the V1 and V2 ROIs were limited to regions of low curvature. The profiles taken through the gray matter are shown schematically in Figure 4B. Because the greatest amount of striate was evident in the images taken perpendicular to the calcarine sulcus (in Subjects 1-4), all image profiles were defined in this view. Figure 4C shows the intensity profiles for each subject. The averaged profiles through the V1 region are shown in blue (solid line), and those through in the V2 region are in red (dashed line). The number of profiles used in the calculation ("n" in the profile plot) was matched as closely as possible for the V1 and V2 regions for each subject. The left side of the plots represents layer I, adjacent to the CSF, and the right side is layer VI, next to the white matter. All subjects show very similar profiles, even Subject 5, who showed considerably less manually defined striated cortex than the other subjects. The V1 region profiles show a large dip in intensity, suggestive of cortical striation, indicated by the arrows. The profiles from the V2 region also show a small dip in intensity at approximately the same location in the gray matter. However, the size of this intensity change is significantly smaller in V2 than V1 for all subjects ($p < 10^{-9}$).

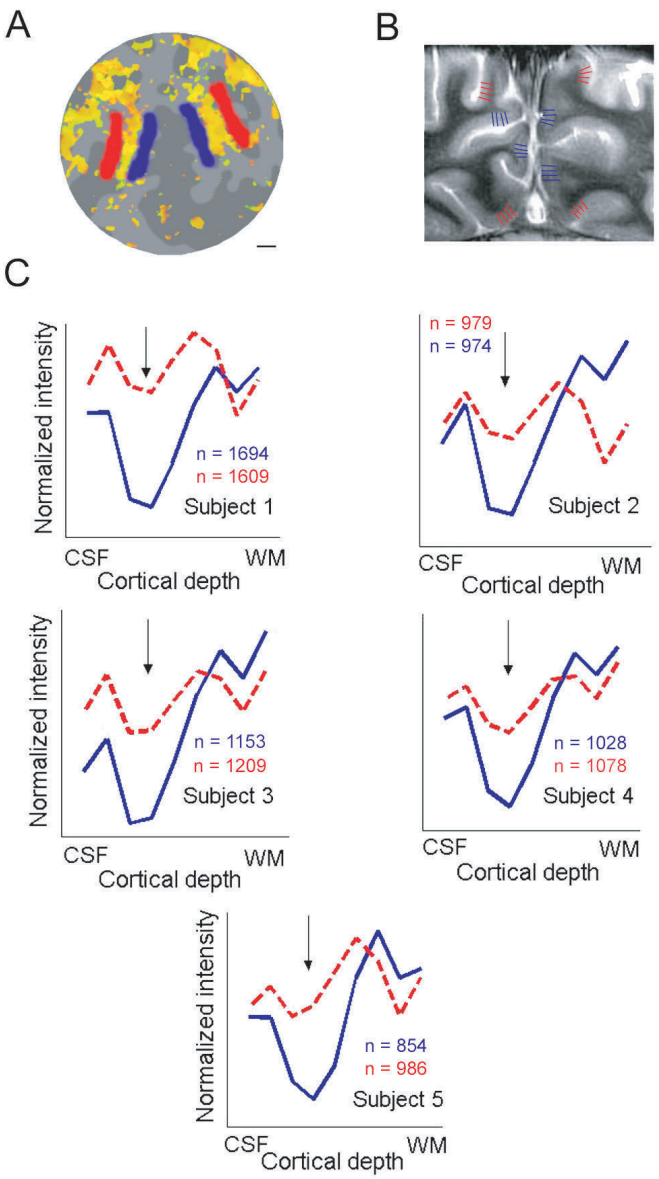

Figure 4. Intensity profiles taken from regions of V1 and V2 adjacent to the functionally mapped vertical meridian. A shows an example of the regions used for measuring the intensity profiles, and B shows these regions on the high-resolution image. C shows the V1 (blue, solid line) and V2 (red, dashed line) profiles averaged over these regions for each of the five subjects. The left side of the plots corresponds to cerebrospinal fluid (CSF), and WM is the white matter. The arrow shows the location of the hypointense band indicative of cortical striation for each subject. The number of profiles used for each plot are given by "n" (blue, V1; red, V2).

Discussion

In all subjects scanned for this study, we found a good correspondence between the borders of V1 defined functionally using fMRI and anatomically by cortical striation consistent with the stria of Gennari. This is the first time that a correspondence between the retinotopically defined V1 and anatomically defined striate cortex has been demonstrated in individual subjects in vivo.

This correspondence between the boundaries of anatomical striate cortex and functional mapping of the vertical meridian in single human subjects is important for several reasons. First, it validates two recently developed methodologies: high-resolution structural MR and quantitative fMRI mapping of visual fields. Second, it opens up the possibility of applying these techniques to other areas where the outcome is not so strongly expected. Third, the ability to carry out these procedures in single subjects establishes the possibility of using anatomical identification of cortical regions as a platform on which to build studies of individual differences.

Possible sources of error

There are several possible sources of error in the comparison of data collected with differing methodologies that have potentially adverse affects on the establishment of anatomical and functional correspondence. First, the structural MRI demands very high spatial resolution and the functional MRI demands high temporal resolution (on the order of seconds). It is therefore not possible to acquire the data sets at the same spatial resolution. In this case, the anatomical resolution is 0.3 x 0.3 x 1.5 mm^3, compared to the functional resolution of 2 x 2 x 2 mm^3. Although this means that the spatial accuracy of the fMRI data is likely to be less than that of the structural data, this should not lead to any systematic offset between the two datasets. Secondly, EPI can suffer from image distortions in regions of the brain where steep magnetic susceptibility changes occur. This means that image registration between the two data sets of different contrast, resolution, and possibly distortion may not be perfect. Distortion of EPI images in the region of the visual cortex, however, is very low, because it is far from the major sinuses that typically cause problems. Furthermore, because we are only acquiring EPI images in the occipital lobe, the risk of propagating registration errors that often occur in the frontal and temporal regions is reduced.

A further source of error in the data presented here results from the use of human observers for the manual identification of cortical striation in the high-resolution anatomical images. While using this subjective approach led to variations in the amount of striate cortex detected (60% of the striate cortex identified by two of the three observes was identified by all three observers), this method is also very sensitive to detecting the cortical myelination in regions where changing resolution, signal-to-noise ratio, and cortical curvature make automated methods fail. The current algorithms for nondirected, computer-based identification of the striate cortex on this complex 3D data have not, in our experience, been sensitive enough to reliably detect the boundaries. This is an area where advances in cortical segmentation and modeling will potentially have a significant impact.

Variation between subjects

The first hypothesis presented in the Introduction was that a large percentage of the functionally defined V1 should show an anatomical striation. Although this is obviously the case for Subject 1, it can be seen from Figure 3 that there is considerable variation in this measure between the five subjects. There are two main explanations for these differences: image quality and differences in patterns of cortical folding. The differences in image quality can be seen in Figure 1: The images from Subjects 4 and 5 are much less clear than the other subjects. The quality varies with the signal-noise ratio in a particular session and the amount of subject movement. There is a significant correlation between the mean signal-noise ratio for the three anatomical scans and the total amount of striated cortex detected ($r = .88$; $n = 5$; $p < .05$). Signal-noise therefore accounts for approximately 77% of the inter-subject variance in the total amount of striated cortex detected. Variation in the signal-noise ratio from subject to subject appears to depend on the position of the head relative to the surface coils. The occipital cortex in Subject 5, for example, is significantly further from the coils than in other subjects. This subject shows a considerably lower signal-noise ratio (42.7) than the other four subjects (mean = 63.6; stdev = 9.3). Because the distance from the coil depends on the size and shape of the subject's head, it is difficult to adjust for. Additionally, the small in-plane voxel size means that even a small amount of head movement can blur the image. Thus, the amount of striated cortex detected will also depend on how still the subject remained while in the scanner.

Because our image voxels are not isotropic, the resolution of the imaging through the gray matter will vary, depending on the exact orientation of the cortical surface. The range is from 0.3 mm (in-plane voxel size) to 1.5 mm (slice thickness). Because the stria of Gennari is only around 280-μm thick (von Economo & Koskinas, 1929), it will not be possible to visualize an intensity change at a resolution of 1.5 mm. For a given subject, the amount and location of cortex that is imaged at the in-plane voxel size will vary depending on the slice orientation used.

In addition to the variation due to the particular folding of the cortex for an individual subject, it is also apparent that striated cortex is rarely detected deep in the calcarine sulcus. This can been seen from the flattened images in Figure 3. The phenomenon is obvious in the anatomical images themselves, and is therefore not an artifact introduced by the registration and transformation processes. A similar pattern was found by Clark et al. (1992) in MR images, but it is not a feature of histologically stained sections. The reasons for the lack of visible striated cortex are not yet clear and require further investigation.

Cortical striation outside V1

Over 95% of the cortical striation that was identified in the five subjects lies within the functional border of V1 as defined by the vertical meridian. Small patches of cortical striation were identified outside of V1. Clarke and Miklossy (1990) showed that V2 has a very similar myelination pattern to V1, but that the myelination was less distinct than the stria of Gennari. The V2 intensity profiles in Figure 4 are consistent with this finding. All subjects show a small dip in intensity (indicating white matter) at a similar position to the much larger dip in the V1 profiles.

The most likely explanation for the identification of cortical striation outside of V1 is that the observers searching for hypointensity bands in the images are detecting this fainter myelination of V2. The signal-noise ratio varies considerably across these high-resolution images. If it were particularly high in an area of V2, and the partial voluming effects were absent, any change in image intensity would be

more readily detectable. The manual identification method that we have used here does not allow a quantification of the strength of myelination. Ideally, the detection of striated cortex would be fully automated to allow for such quantification, but this is challenging due to large variations in image intensity and contrast within a scan.

Future applications of high-resolution anatomical scanning

Mapping of the foveal confluence of V1/V2/V3

Retinotopic mapping of the visual areas is still growing in popularity, and is now an indispensable tool for visual fMRI. However, as Dougherty et al. (2003) point out, it is still very challenging to functionally map the central fovea with this technique. In this region, the early visual areas have a "shared" foveal representation. With careful selection of slice orientation, it should be possible to map out this very posterior region of striate cortex using high-resolution anatomical imaging of the myeloarchitecture. Such a technique would be useful for the investigation of high-acuity visual processing that requires the central fovea.

Definition of higher visual areas

The stria of Gennari is one of the best-defined patterns of myelination in the cortex, and the demonstration that anatomically defined striate cortex corresponds to the functional definition of V1 measured with fMRI is not too surprising. However, there are many other brain areas, both visual and nonvisual with distinct myelination patterns, which cannot be so readily identified functionally with simple stimuli. Exploitation of this high-resolution methodology could aid the definition of these areas. However, to make the more subtle distinction required for such identification, it will be necessary to develop methodology for automatic detection of the intensity changes in the image. Schleicher et al. (2000) have developed such a system for postmortem brains, although the image quality can be significantly better because they can be scanned for considerably longer than human subjects.

Investigation of abnormal visual systems

Several studies have recently investigated the functional organization of the occipital lobe in congenitally blind humans (Amedi, Malach, Hendler, Peled, & Zohary, 2001; Amedi, Raz, Pianka, Malach, & Zohary, 2003; Gizewski, Gasser, de Greiff, Boehm, & Forsting, 2003; Sadato et al., 1996). These studies have described an altered function in the occipital lobe, in particular the representation of Braille reading. In addition, Amedi et al. (2003) suggest that the "early" visual cortex is activated in response to verbal memory. In these subjects, although the calcarine sulcus can be a guide to the location of area 17, there is considerable variability in the location and size of this region even in normal, sighted subjects. Obviously, a functional definition based on retinotopic mapping cannot be performed, so the ability to anatomically define different areas would allow direct comparisons between the altered and normal occipital lobes.

Conclusion

We have shown that there is an excellent correspondence between the anatomical and functional definitions of V1 in human visual cortex in vivo. This result both provides a validation of the retinotopic mapping technique commonly used in fMRI and suggests that high-resolution imaging of myeloarchitecture may allow anatomical identification of cortical areas in the near future.

Acknowledgments

Both Holly Bridge and Stuart Clare contributed equally to the work. This research was supported by the MRC and The Wellcome Trust. HB is a Royal Society Dorothy Hodgkin Fellow.

Commercial relationships: none.
Corresponding author: Holly Bridge.
Email: holly.bridge@physiol.ox.ac.uk.
Address: FMRIB Centre, John Radcliffe Hospital, Headington, Oxford, OX3 9DU, UK.

References

Amedi, A., Malach, R., Hendler, T., Peled, S., & Zohary, E. (2001). Visuo-haptic object-related activation in the ventral visual pathway. *Nature Neuroscience, 4*(3), 324-330. [PubMed]

Amedi, A., Raz, N., Pianka, P., Malach, R., & Zohary, E. (2003). Early 'visual' cortex activation correlates with superior verbal memory performance in the blind. *Nature Neuroscience, 6*(7), 758-766. [PubMed]

Amunts, K., Malikovic, A., Mohlberg, H., Schormann, T., & Zilles, K. (2000). Brodmann's areas 17 and 18 brought into stereotaxic space-where and how variable? *Neuroimage, 11*(1), 66-84. [PubMed]

Andrews, T. J., Halpern, S. D., & Purves, D. (1997). Correlated size variations in human visual cortex, lateral geniculate nucleus, and optic tract. *The Journal of Neuroscience, 17*(8), 2859-2868. [PubMed]

Barbier, E. L., Marrett, S., Danek, A., Vortmeyer, A., van Gelderen, P., Duyn, J., et al. (2002). Imaging cortical anatomy by high-resolution MR at 3.0T: Detection of the stripe of Gennari in visual area 17. *Magnetic Resonance in Medicine, 48*(4), 735-738. [PubMed]

Clark, V. P., Courchesne, E., & Grafe, M. (1992). In vivo myeloarchitectonic analysis of human striate and extrastriate cortex using magnetic resonance imaging. *Cerebral Cortex, 2*(5), 417-424. [PubMed]

Clarke, S., & Miklossy, J. (1990). Occipital cortex in man: Organization of callosal connections, related myelo- and cytoarchitecture, and putative boundaries of functional visual areas. *Journal of Comparative Neurology, 298*(2), 188-214. [PubMed]

DeYoe, E. A., Carman, G. J., Bandettini, P., Glickman, S., Wieser, J., Cox, R., et al. (1996). Mapping striate and extrastriate visual areas in human cerebral cortex. *Proceedings of the National Academy of Sciences U. S. A., 93*(6), 2382-2386. [PubMed][Article]

Dougherty, R. F., Brewer, A. A., Koch, V., Fischer, B., Modersitzki, J., & Wandell, B. A. (2003). The position, surface area and visual field representation of visual areas V1/2/3 in human visual cortex. *Journal of Vision, 3*(10), 586-598, http://journalofvision.org/3/10/1/, doi:10.1167/3.10.1. [PubMed][Article]

Engel, S. A., Glover, G. H., & Wandell, B. A. (1997). Retinotopic organization in human visual cortex and the spatial precision of functional MRI. *Cerebral Cortex, 7*(2), 181-192. [PubMed]

Engel, S. A., Rumelhart, D. E., Wandell, B. A., Lee, A. T., Glover, G. H., Chichilnisky, E. J., & Shadlen, M. N. (1994). fMRI of human visual cortex. *Nature, 369*(6481), 525. [PubMed]

Gennari, F. (1782). Francisci Gennari Parmensis Medicinae Doctoris Collegiati de Peculiari Structura Cerebri Nonnullisque Eius Morbis-Paucae Aliae Anatom. Observat. Accedunt. Parma, Italy: Regio Typographeo.

Gizewski, E. R., Gasser, T., de Greiff, A., Boehm, A., & Forsting, M. (2003). Cross-modal plasticity for sensory and motor activation patterns in blind subjects. *NeuroImage, 19*(3), 968-975. [PubMed]

Hadjikhani, N., Liu, A. K., Dale, A. M., Cavanagh, P., & Tootell, R. B. (1998). Retinotopy and color sensitivity in human visual cortical area V8. *Nature Neuroscience, 1*(3), 235-241. [PubMed]

Huk, A. C., Dougherty, R.F., & Heeger, D. J. (2002). Retinotopy and functional subdivision of human areas MT and MST. *The Journal of Neuroscience, 22*(16), 7195-205. [PubMed]

Jenkinson, M., Bannister, P., Brady, M., & Smith, S. (2002). Improved optimization for the robust and accurate linear registration and motion correction of brain images. *NeuroImage, 17*(2), 825-841. [PubMed]

Nestares, O., & Heeger, D. J. (2000). Robust multiresolution alignment of MRI brain volumes. *Magnetic Resonance in Medicine, 43*(5), 705-715. [PubMed]

Sadato, N., Pascual-Leone, A., Grafman, J., Ibanez, V., Deiber, M. P., Dold, G., & Hallett, M. (1996). Activation of the primary visual cortex by Braille reading in blind subjects. *Nature, 380*(6574), 526-528. [PubMed]

Schleicher, A., Amunts, K., Geyer, S., Kowalski, T., Schormann, T., Palomero-Gallagher, N., & Zilles, K. (2000). A stereological approach to human cortical architecture: Identification and delineation of cortical areas. *Journal of Chemical Neuroanatomy, 20*(1), 31-47. [PubMed]

Sereno, M. I., Dale, A. M., Reppas, J. B., Kwong, K. K., Belliveau, J. W., Brady, T. J., et al. (1995). Borders of multiple visual areas in humans revealed by functional magnetic resonance imaging. *Science, 268*(5212), 889-893. [PubMed]

Smith, A. M., Lewis, B. K., Ruttimann, U. E., Ye, F. Q., Sinnwell, T. M., Yang, Y., et al. (1999). Investigation of low frequency drift in fMRI signal. *Neuroimage, 9*(5), 526-533. [PubMed]

Stensaas, S. S., Eddington, D. K., & Dobelle, W. H. (1974). The topography and variability of the primary visual cortex in man. *Journal of Neurosurgery, 40*, 747-755. [PubMed]

Teo, P. C., Sapiro, G., & Wandell, B. A. (1997). Creating connected representations of cortical gray matter for functional MRI visualization. *IEEE Transactions on Medical Imaging, 16*(6), 852-863. [PubMed]

Tootell, R. B., & Taylor, J. B. (1995). Anatomical evidence for MT and additional cortical visual areas in humans. *Cerebral Cortex, 5*(1), 39-55. [PubMed]

von Economo, C. F., & Koskinas, G. N. (1929). *The Cytoarchitectonics of the Human Cerebral Cortex.* London: Oxford University Press.

Wade, A. R., Brewer, A. A., Rieger, J. W., & Wandell, B. A. (2002). Functional measurements of human ventral occipital cortex: Retinotopy and colour. *Philosophical Transactions of the Royal Society of London B Biological Sciences, 357*(1424), 963-973. [PubMed]

Walters, N. B., Egan, G. F., Kril, J. J., Kean, M., Waley, P., Jenkinson, M., & Watson, J. D. (2003). In vivo identification of human cortical areas using high-resolution MRI: An approach to cerebral structure-function correlation. *Proceedings of the National Academy of Sciences U. S. A., 100*(5), 2981-2986. [PubMed][Article]

Wandell, B. A., Chial, S., & Backus, B. T. (2000). Visualization and measurement of the cortical surface. *Journal of Cognitive Neuroscience, 12*(5), 739-752. [PubMed]

Watson, J. D., Myers, R., Frackowiak, R. S., Hajnal, J. V., Woods, R. P., Mazziotta, J. C., et al. (1993). Area V5 of the human brain: Evidence from a combined study using positron emission tomography and magnetic resonance imaging. *Cerebral Cortex, 3*(2), 79-94. [PubMed]

Zeki, S., Watson, J. D., Lueck, C. J., Friston, K. J., Kennard, C., & Frackowiak, R. S. (1991). A direct demonstration of functional specialization in human visual cortex. *The Journal of Neuroscience, 11*(3), 641-649. [PubMed]

Zeki, S. M. (1970). Interhemispheric connections of prestriate cortex in monkey. *Brain Research, 19*(1), 63-75. [PubMed]

Zhang, Y., Brady, M., & Smith, S. (2001). Segmentation of brain MR images through a hidden Markov random field model and the expectation-maximization algorithm. *IEEE Transactions on Medical Imaging, 20*(1), 45-57. [PubMed]